EPJ Web of Conferences **158**, 03007 (2017)
QFTHEP 2017
DOI: 10.1051/epjconf/201715803007

Recent measurements of $K^{\pm}_{l3}$ form factors at NA48

Sergey Shkarovskiy[1,⋆] on behalf of the NA48/2 Collaboration

[1] *Joint Institute for Nuclear Research, Joliot-Curie, 6 Dubna, Moscow region, Russia, 141980*

Abstract. The NA48/2 experiment presents a final result of the charged kaon semileptonic decays form factors measurement based on 4.28 million $K^{\pm}_{e3}$ and 2.91 million $K^{\pm}_{\mu 3}$ selected decays collected in 2004. The result is competetive with other measurements in $K^{\pm}_{\mu 3}$ mode and has a smallest uncertainty for $K^{\pm}_{e3}$, that leads to the most precise combined $K^{\pm}_{l3}$ result and allows to reduce the form factor uncertainty of $|V_{US}|$.

1 Introduction

The main purpose of the NA48/2 experiment at the CERN SPS was a search for the direct CP violation in $K^{\pm}$ decay to three pions [1]. The experiment used simultaneous K^{+} and K^{-} beams with momenta of 60 GeV/c propagating through the detector along the same beam line. Data were collected in 2003-2004, providing the large samples of reconstructed $K^{\pm} \to 3\pi$ decays and a high precision data for many rare kaon decay studies. The layout of beams and detectors is shown in Fig. 1.

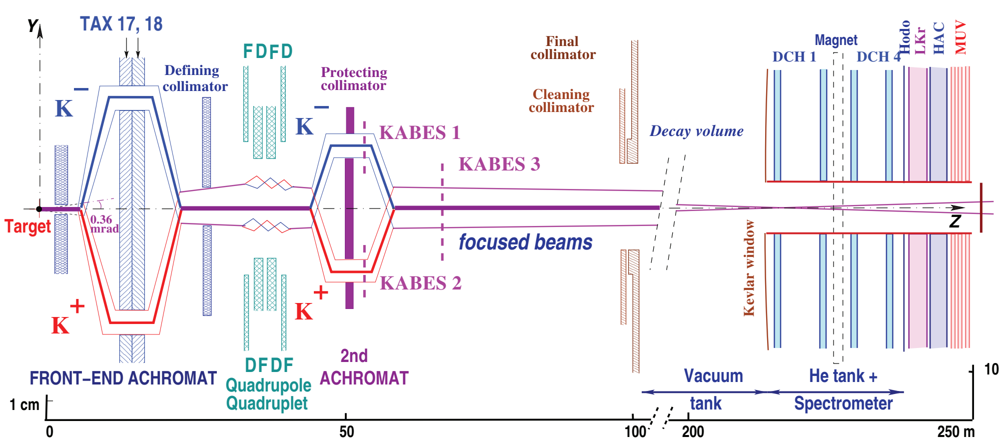

Figure 1. Schematic side view of the NA48/2 beamline and detectors.

Apart from that, a large statistics of $K^{\pm} \to \pi^{0} l^{\pm} \nu$ (K_{l3}) events has been collected during a special data taking period of 2004 (l means e or μ lepton). Semileptonic kaon decays (K_{l3}) offer the most

⋆e-mail: Sergey.Shkarovskiy@cern.ch

precise determination of the CKM matrix element $|V_{US}|$ [2], that require both a branching ratio and a formfactors experimental measurement. The K_{l3} precision form factors measurement results based on the NA48/2 data analysis are presented in this paper.

The K_{l3} decay width in the absence of electromagnetic effects can be represented by the Dalitz plot density depending on the lepton and pion energies in kaon rest frame E_l and E_π respectively [3]:

$$\frac{d^2\Gamma_0(K_{l3})}{dE_l dE_\pi} = N(Af_+^2(t) + Bf_+(t)f_-(t) + Cf_-^2(t)), \tag{1}$$

where $t = (P_K - P_\pi)^2 = m_K^2 + m_\pi^2 - 2m_K E_\pi$, N is a normalization constant and $f_-(t) = (f_+(t) - f_0(t))(m_K^2 - m_{\pi+}^2)/t$. Here $f_+(t)$ and $f_0(t)$ are the so called vector and scalar K_{l3} form factors, respectively. The m_K is a mass of charged kaon m_π is a mass of neutral pion and $m_{\pi+}$ is a mass of charged pion.

Kinematical factors in the (1) expression are:

$$A = m_K(2E_l E_\nu - m_K(E_\pi^{max} - E_\pi)) + m_l^2((E_\pi^{max} - E_\pi)/4 - E_\nu)$$
$$B = m_l^2(E_\nu - (E_\pi^{max} - E_\pi)/2)$$
$$C = m_l^2(E_\pi^{max} - E_\pi)/4,$$

where $E_\pi^{max} = (m_K^2 + m_\pi^2 - m_l^2)/(2m_K)$ (m_l is the lepton mass), and $E_\nu = m_K - E_l - E_\pi$ is a neutrino energy in the kaon rest frame. For K_{e3} the terms B and C are negligible due to the small electron mass, so in this case in fact only the vector form factor participates in the Dalitz plot description.

	$f_+(t)$	$f_0(t)$
Quadratic	$1 + \lambda'_+ t/m_\pi^2 + \frac{1}{2}\lambda''_+(t/m_\pi^2)^2$	$1 + \lambda'_0 t/m_\pi^2$
Pole	$\frac{M_V^2}{(M_V^2 - t)}$	$\frac{M_S^2}{(M_S^2 - t)}$
Dispersive	$\exp\left(\frac{(\Lambda_+ + H(t))t}{m_\pi^2}\right)$	$\exp\left(\frac{(ln[C] - G(t))t}{(m_K^2 - m_\pi^2)}\right)$

Table 1. Definitions of the form factor parameterizations used in the analysis

Definitions of the implemented parameterizatios are shown in the Table 1: the Quadratic [4] parameterization (fit parameters $\lambda'_+, \lambda''_+, \lambda'_0$), the Pole [5] (fit parameters M_V, M_S) and the Dispersive [6] one (fit parameters $\Lambda_+, ln[C]$).

2 Beams and detectors

A detailed descriptions of the detector elements and beam line are available in [1, 7]. The NA48/2 experiment used two simultaneous beams produced by 400 GeV/c protons impinging on a berillium target. Particles of opposite charge with a central momentum of 60 GeV/c and a momentum band of ±3.8% (RMS) were selected by a system of dipole magnets, focusing quadrupoles, muon sweepers and collimators. Two beams with an opposite charges were split in the vertical plane and than recombined on a common axis. The decay volume was a 114 m long vacuum tank.

Charged particles from $K^\pm$ decays were measured by a magnetic spectrometer (DCH) that included four drift chambers (DCH1–DCH4) and a dipole magnet between DCH2 and DCH3. The spectrometer momentum resolution was $\sigma(P)/P = 1.02\% \oplus 0.044\%P$, where P is a charged particle momentum in GeV/c. The magnetic spectrometer was followed by a scintillator hodoscope (HOD) consisting of two planes segmented into horizontal and vertical strips and arranged in four quadrants.

 DOI: 10.1051/epjconf/201715803007

A liquid Krypton calorimeter (LKr) [8] was used to reconstruct $\pi^0 \to \gamma\gamma$ decays. It was an almost homogeneous ionization chamber with an active volume of $\sim$ 10 m^3 of liquid krypton, segmented transversally into 2 cm × 2 cm projective cells. The calorimeter was 27 X_0 thick and has an energy resolution $\sigma(E)/E = 0.032/\sqrt{E} \oplus 0.09/E \oplus 0.0042$ (E in GeV). The space resolution for a single electromagnetic shower can be parameterized as $\sigma_x = \sigma_y = 0.42/\sqrt{E} \oplus 0.06$ cm both for X and Y coordinates.

The LKr was followed by a hadronic calorimeter with a total iron thickness of 1.2 m. A muon detector (MUV) was located further downstream. It consisted of three planes of scintillator strips, each preceded by a 80 cm thick iron wall. The strips were aligned horizontally in the first and last planes, and vertically – in the second plane. They were 2.7 m long and 2 cm thick, and read out by photomultipliers at both ends.

3 Events reconstruction and selection

The data used for the form factor (FF) analysis were collected in 2004 during a dedicated run with a special trigger setup which required at least one charged track crossing the Hodoscope HOD and an energy deposit of at least 10 GeV in the electromagnetic calorimeter. Nearly 480×10^6 triggered events have been recorded during the special short period.

3.1 π^0 selection

The event is considered as a preliminary candidate to K_{l3} decays, if it contains at least 2 LKr clusters consistent with a photons of reconstructed energy above 3 GeV (good photons). Fiducial cuts on the minimum distance between the good photon and LKr edges or centre are applied in order to avoid elecromagnetic showers energy loss. In addition, a minimum distance between the good photon and the nearest LKr cell with a known readout problems (dead cell) is required to be at least 2 cm. The minimum distance from the selected photon to any in-time (within 10 ns) charged track impact point at LKr front face is 15 cm, and the minimum distance to any other in-time (within 5 ns) cluster is 10 cm.

Each pair of the close in time (within 5 ns) good photons forms a π^0 candidate, if there is no extra good photons in ±5 ns vicinity of the two π^0 photons average time. This extra-photons cut suppresses $\pi^\pm\pi^0\pi^0$ background. A distance between π^0 photons on LKr is required to be more than 20 cm, and the minimum sum of two photon energies is 15 GeV. So high energy threshold ensures a high efficiency of $E_{LKr} > 10$ GeV trigger requirement.

Longitudinal K_{l3} decay position Z_n (neutral vertex Z coordinate) is defined as a longitudinal position of π^0 decay, reconstructed from LKr data assuming PDG [9] value for π^0 mass.

3.2 Charged leptons selection

A candidate to K_{l3} decay is required to contain, apart from the reconstructed π^0, also at least one reconstructed DCH track of charged particle with a minimum momentum of 5 GeV/c. A harder muon momentum cut $P\mu >= 10$ GeV/c is applied in the case of muon positive identification in order to ensure high MUV efficiency. A distance from the track impact point on the LKr front face to the closest dead cell is required to be above 2 cm, and a minimum distance from the nominal beam axis to the reconstructed track at each DCH plane is 15 cm. A track is required to be in-time with the reconstructed π^0 within 10 ns, and no extra good tracks are allowed to be close in time to the considered track (within 8 ns).

Track with $2.0 > E/P > 0.9$ is identified as an electron from K_{e3} decay. For experimental data, if $E/P < 0.9$ and there is a MUV muon candidate associated to the track, it is identified as a muon from $K_{\mu 3}$ decay.

3.3 Kaon momentum

Kaon momentum is measured ignoring the possible real radiative photons, so this radiative effect is treated just as an extra source of measurement error.

For the kaon momentum measurement we direct Z axis along the beam average position in space, measured from $3\pi^{\pm}$ data. In the assumptions of zero neutrino mass and kaon flight along the beam axis (that means availability of the measured neutrino transverse momentum $P_T(\nu) = -P_t$), two solutions of quadratic equation for kaon momentum P_K exist:

$$P_K = P_{1,2} = (\phi P_Z \pm \sqrt{d})/(E^2 - P_Z^2), \tag{2}$$

where

$$\phi = 0.5(M_K^2 + E^2 - P_t^2 - P_Z^2);$$
$$d = \phi^2 P_Z^2 - (E^2 - P_Z^2)(M_K^2 E^2 - \phi^2)),$$

and E, P_t, P_Z are the total energy and total momentum of all the registered particles π^0, l.

An average beam momentum P_B is known from $3\pi^{\pm}$ decays data. For each event, both for K_{e3} and $K_{\mu 3}$ selections a combination with the minimum $\Delta P = |P_K - P_B|$ is chosen as the best candidate. Finally, a cut on the reconstructed kaon momentum is applied: $-7.5\ GeV/c < (P_K - P_B) < 7.5\ GeV/c$.

3.4 Background suppression cuts

For the clean K_{e3} selection one need to reject the $K^{\pm} \to \pi^{\pm}\pi^0$ decays with a $\pi^{\pm}$ misidentified as e due to the rare occasional high enegry deposit in LKr, resulting in $E/P > 0.9$. Reconstructed transversal momentum for these background events doesn't depend on the charged particle mass and should be close to zero. So a requirement on the reconstructed neutrino transverse momentum is applied: $P_t(\nu) >= 0.03\ GeV/c$, that takes into account both the effect of resolution and the beam angular spread influence.

For $K_{\mu 3}$ selection, an essential background may come from $K^{\pm} \to \pi^{\pm}\pi^0$ decays with a subsequent $\pi^{\pm} \to \mu^{\pm}\bar{\nu}$ process. In order to suppress this background, we remove the cases, when a kaon mass can be well reconstructed in the assumption of 2π kaon decay – by means of the requirement of $m(\pi^{\pm}\pi^0) < 0.47\ GeV/c^2$. Additionally, an empirically found cut $m(\pi^{\pm}\pi^0) < (0.6 - P_t(\pi^0))\ GeV/c^2$ (P_t in GeV/c) improves the suppression of 2π background further.

Also for $K_{\mu 3}$, we suppress the possibility of successfull $\pi^{\pm} \to \mu^{\pm}\bar{\nu}$ reconstruction by the requirement on the minimum dilepton invariant mass $m(\mu\bar{\nu}) > 0.18\ GeV/c^2$, that is well above $m(\pi^+)$. The majority of background events rejected by this cut are also rejected by the above empirical $P_t(\pi^0)$)-dependent cut, that makes its nature more clear – in both cases we reject the $K^{\pm} \to \pi^0(\pi^{\pm} \to \mu^{\pm}\bar{\nu})$ background events with a muon that conserves approximately the momentum of its parent pion. Nevertheless, these two cuts suppress the tails of background distribution in a somewhat different ways, so we apply both.

For both $K_{\mu 3}$ and K_{e3} samples the $K^{\pm} \to \pi^{\pm}\pi^0\pi^0$ decays can contribute to the background, if two γ clusters from π^0 are not detected and if the charged pion is misidentified as electron (for K_{e3}), or if the pion decays into muon and neutrino (for $K_{\mu 3}$). It has been found, that for this background source

 DOI: 10.1051/epjconf/201715803007

a difference between two possible solutions (2) of quadratic equation for P_K is relatively large. So for the $K_{\mu 3}$ events selection we apply a requirement of $|P_2 - P_1| < 60 GeV$. For K_{e3} events such a cut also can suppress the 3π source of background, but even without this suppression our K_{e3} selection is rather clean. The loss of the signal statistics caused by this cut is not justified in K_{e3} case, so we don't apply this cut for K_{e3} selection.

3.5 $P_L(\nu)^2$ cut

One can evaluate from kinematics of K_{l3} decay reconstruction, that the physical reason of two-fold P_K uncertainty is in fact the unknown sign of true longitudinal neutrino momentum $p_L(\nu)$ in the kaon center of mass system.

When the measured value of $P_L(\nu)^2 = E(\nu)^2 - P_T(\nu)^2$ is negative (and when it is smaller than its resolution) a sign of $P_L(\nu)$ is uncertain. In this case the choice of the best P_K value from two close solutions of quadratic equation becomes arbitrary. As a result, the region of small and negative measured values of $P_L(\nu)^2$ is dominated by the events with an essentially mismeasured $P_L(\nu)^2$ values.

The measurement of $P_L(\nu)^2$ depends on reconstructed $P_T(\nu)^2$, that essentially depends on the assumed direction of kaon filght as well as on the transverse coordinates of the reconstructed decay vertex. As a consequence, the accurate modelling of the kaon momentum choice at small and negative $P_L(\nu)^2$ is sensitive to the fine details of beams geometry, that is problematic for exact simulation.

A comparison between the reconstructed experimental and Monte Carlo $P_L(\nu)^2$ distributions is shown in the Fig. 2. One can see, that there is some discrepance between the data and simulation at small and negative $P_L(\nu)^2$ values. It is not so well visible on the normalized overlapped plots, but the ratios of these distributions show the clear difference of the negative tails, and this difference is larger for K_{e3} decays.

Due to the inevitable residual discrepance between the simulated and real beam geometry, the result of kaon momentum solution choise for the events from the negative $P_L(\nu)^2$ tail essentially depends on the vertex transverse coordinates measurement procedure (CDA or neutral vertex). And even for the neutral vertex we have for K_{e3} a considerable dependence of our results on the minimum $P_L(\nu)^2$ as long as we don't cut at $P_L(\nu)^2 > 0.0014\ (GeV/c)^2$. For a higher cut values all the results remain stable.

For the $K_{\mu 3}$ case no essential variations of our results versus $P_L(\nu)^2$ cut have been observed, and no considerable systematic uncertainty may be linked to the sources of MC/Dtata discrepance. Together with the fact of smaller discrepance in comparison with K_{e3} case, it leads us to the decision not to apply $P_L(\nu)^2$ cut for $K_{\mu 3}$ in order to save signal statistics.

So a special cut has been applied to exclude the K_{e3} events subsample, that introduces a large sensitivity of the results to the precision of beam simulation: $P_L(\nu)^2 > 0.0014\ (GeV/c)^2$. This cut leads to the considerable loss of statistics: K_{e3} one decreases from 6.05 millions to 4.28 millions of events (about 30% are lost). It makes the statistical error larger, but a large systematic uncertainty of complex nature is diminished.

The selected event Dalitz plots with a binning of $5\times5\ MeV$ are shown in the Fig. 3. They are used for all the further fits after correction for residual background. The total statistics of selected data is 4.278×10^6 events for K_{e3}, and 2.907×10^6 events for $K_{\mu 3}$ selection.

4 Monte Carlo simulation and form factor fits

Semileptonic radiative Monte Carlo samples have been simulated with the KLOE generator [10]. It is based on the Dalitz plot density (1) with a linear approximation for the vector form factor $f_+(t) =$

DOI: 10.1051/epjconf/201715803007

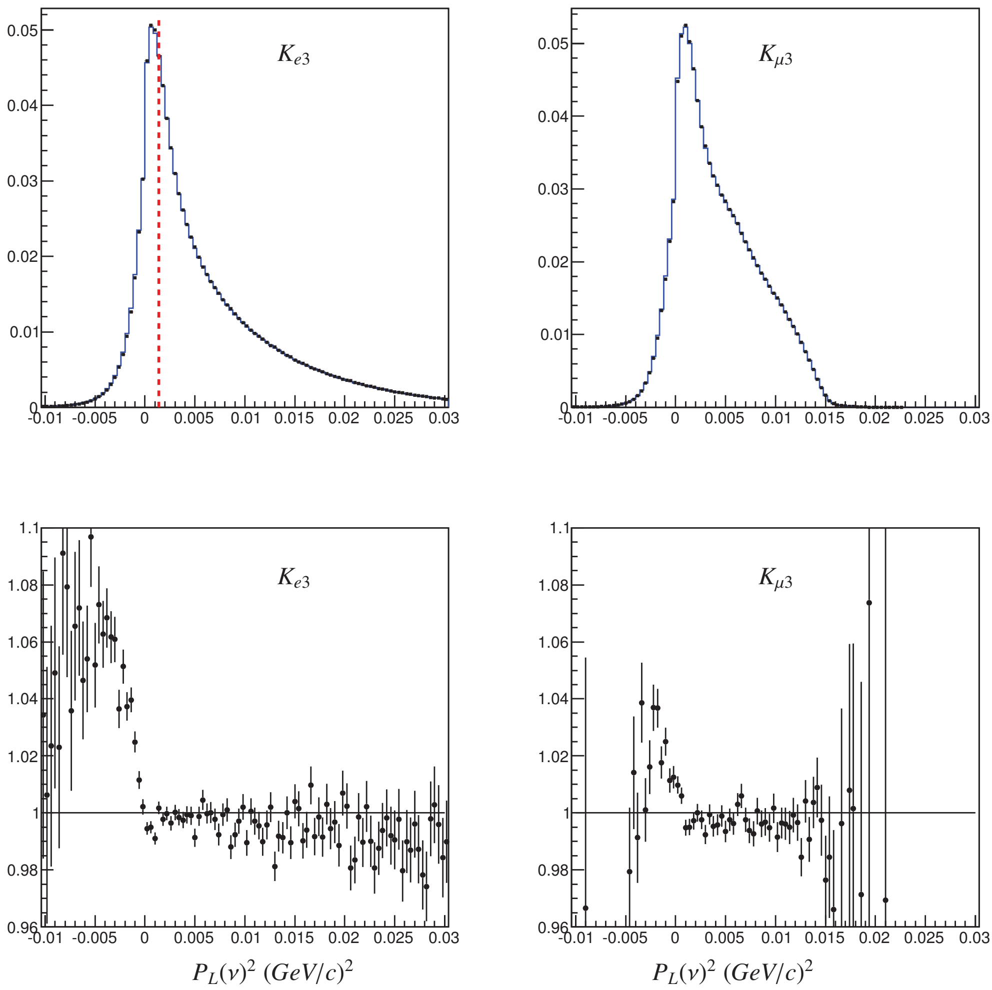

Figure 2. Normalized $P_L(\nu)^2$ distributions for the data (dots) and background-corrected Monte Carlo (histograms). Upper left plot – K_{e3}, upper right – $K_{\mu3}$. Lower plots – the corresponding MC/Data ratios. Vertical dashed line shows the cut applied for the K_{e3} events selection.

$1 + 0.0296 \cdot t/m^2_{\pi+}$ and without negative form factor ($f_- = 0$) for the both cases of semileptonic decay. The simulation codes for two semileptonic modes differ only in the lepton mass value. It corresponds to $f_+(t) = f_0(t)$ assumption for $K_{\mu3}$ simulation. Apart from the Dalitz plot radiative correction, one real radiative photon is simulated for each K_{e3} event as well as for some fraction of $K_{\mu3}$ decays.

We will denote here the Dalitz plot density expression (1) with $N = 1$ and with a form factors written in terms of Quadratic parameterization as $Q_l(E_\pi, E_l, \lambda'_+, \lambda''_+, \lambda'_0)$ for the corresponding K_{l3} case ($l = \mu, e$).

For each fit iteration with the current changed form factor parameters the fitting code reads a special file of selected events data. For each event, a probability to simulate this event with the

DOI: 10.1051/epjconf/201715803007

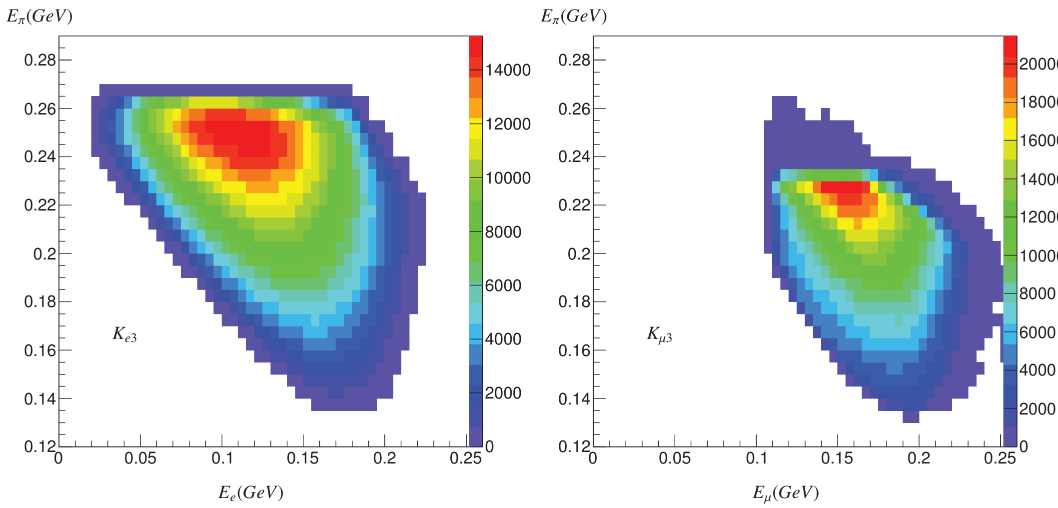

Figure 3. Reconstructed Dalitz plots for K_{e3} (left) and $K_{\mu 3}$ (right) selections of experimental data

Monte Carlo generator [10] $\rho_0^{gen} = Q_l(E_\pi, E_l, 0.0296, 0.0, 0.0296)$is calculated. Than a probability to simulate the same event with the current fit parameters **ff** is also obtained from one of the considered form factor parameterisation $\rho_0^{ff}(E_\pi, E_l, \mathbf{ff})$. The individual event weight $W_{evt} = \frac{\rho_0^{ff}}{\rho_0^{gen}}$ is used in order to fill the simulated Dalitz plot according to the current form factor parameters.

Than, for each fit iteration, χ^2 is calculated from the experimental background-corrected Dalitz plot $D_{i,j}$ and the current Monte-Carlo simulated one $MC_{i,j}$:

$$\chi^2 = \Sigma_{i,j} \frac{(D_{i,j} - MC_{i,j})^2}{(\delta D_{i,j})^2 + (\delta MC_{i,j})^2}, \tag{3}$$

where i, j indices correspond to the cell of Dalitz plot with a center, lying inside the kinematically allowed region for K_{l3} decays without radiative γ [11] and containing at least 20 reconstructed data events. MINUIT [12] package called from the ROOT [13] interface minimizes χ^2 by means of parameters variation, and in such a way the resulting fit parameter values, their errors and correlation coefficients are found.

5 Background

Four kaon decay modes have been considered as a possible sources of residual background for the both semileptonic decays and have been simulated for the present analysis (see Table 2). Additionally, the effect of $K_{\mu 3}$ misidentification as K_{e3} (due to the $\mu \to e\nu$ decay) has been taken into account.

Inner bremsstrahlung part of $\pi^\pm\pi^0\gamma$ decay was simulated separately for the kaon rest frame kinetic energy of the charged pion $T^*_{\pi^\pm} < 90 MeV$, its probability estimation is taken from [14].

The experimental two-dimensional Dalitz plot is corrected for background by subtracting of the estimated background contributions.

Process	Notation	Br	N_g	F_e	F_μ
$K^\pm \to \pi^\pm(\pi^0 \to 2\gamma)$	2π	20.66	393.2	0.270	0.264
$K^\pm \to \pi^\pm 2(\pi^0 \to 2\gamma)$	3π	1.761	62.5	0.286	1.833
$K^\pm \to \pi^\pm(\pi^0 \to e^+e^-\gamma)$	$2\pi D$	1.174	1.5	0.049	0.000
$K^\pm \to \pi^\pm\gamma(\pi^0 \to 2\gamma)$	$2\pi\gamma$	0.0275	35.3	0.004	0.044
$K^\pm \to \pi^0\mu^\pm\nu(\mu \to e\nu)$	$K^e_{\mu3}$	0.03353	174.3	0.004	0.000

Table 2. Simulated background processes, their probabilities Br (in %), generated MC statistics N_g (in 10^6 events) and the estimated fractions F_e and F_μ (both in units of per mill) in K_{e3} and $K_{\mu3}$ samples for the present selection.

6 Form factor results

Fit results and contributions to systematic uncertainty for Quadratic, Pole and Dispersive Parameterisation are shown in the Table 3.

Quadratic	λ'_+	λ''_+	λ_0
$K_{\mu3}$	$23.32 \pm 3.08_{stat} \pm 3.50_{syst}$	$2.14 \pm 1.06_{stat} \pm 0.96_{syst}$	$14.33 \pm 1.11_{stat} \pm 1.25_{syst}$
K_{e3}	$23.52 \pm 0.78_{stat} \pm 1.29_{syst}$	$1.60 \pm 0.30_{stat} \pm 0.39_{syst}$	
K_{l3}	$23.35 \pm 0.75_{stat} \pm 1.23_{syst}$	$1.73 \pm 0.29_{stat} \pm 0.41_{syst}$	$14.90 \pm 0.55_{stat} \pm 0.80_{syst}$
Pole	m_V	m_S	
$K_{\mu3}$	$879.1 \pm 8.1_{stat} \pm 13.5_{syst}$	$1196.4 \pm 18.1_{stat} \pm 28.8_{syst}$	
K_{e3}	$896.8 \pm 3.4_{stat} \pm 7.6_{syst}$		
K_{l3}	$894.3 \pm 3.2_{stat} \pm 5.4_{syst}$	$1185.5 \pm 16.6_{stat} \pm 35.5_{syst}$	
Dispersive	Λ_+	$ln[C]$	
$K_{\mu3}$	$23.55 \pm 0.50_{stat} \pm 0.97_{syst}$	$186.68 \pm 5.12_{stat} \pm 9.23_{syst}$	
K_{e3}	$22.54 \pm 0.20_{stat} \pm 0.62_{syst}$		
K_{l3}	$22.67 \pm 0.18_{stat} \pm 0.55_{syst}$	$186.12 \pm 4.91_{stat} \pm 11.09_{syst}$	

Table 3. Fit results for the Quadratic ($\times 10^3$), Pole (MeV/c^2) and Dispersive ($\times 10^3$) Parameterisation

The NA48/2 is the first experiment measuring the FF using both K^+ and K^-. In $K_{\mu3}$ the result is dominated by the statistical error, for K_{e3} by the systematic. The NA48/2 K_{e3} and $K_{\mu3}$ in agreement within each other and our combined results are competitive with the current world average.

In order to avoid the problem of partially correlated systematic uncertainties in the K_{e3} and $K_{\mu3}$ results averaging, we just repeated the complete analysis considering the two decay modes information as the joint data set, containing two Dalitz plots that should be simultaneousely fitted with a common form factor parameters.

The final results of the fit for quadratic, pole and dispersive parametrizations are listed in Table 3. The comparison between K_{l3} quadratic fit results by recent experiments is shown in Fig. 6. The 68% confidence level contours are displayed for both K^0_{l3} (KLOE, KTeV and NA48) and charged kaon decays (ISTRA+ studied K^-_{l3} only). The final NA48/2 results presented here are the first high precision measurements done with both K^+ and K^- decays. All the measured parameters are in good agreement with the measurements done by the other experiments.

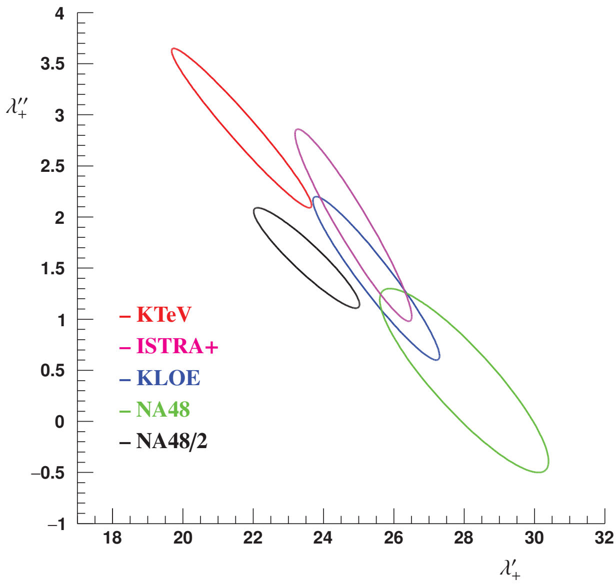

Figure 4. (Color online) 1σ confidence contours for measurements of K_{e3} vector form factor parameters. NA48/2 : result of the present work.

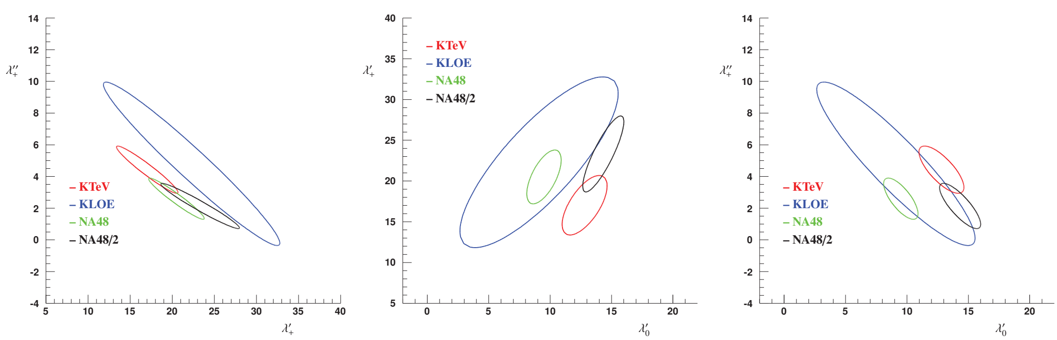

Figure 5. (Color online) 1σ confidence contours for measurements of $K_{\mu 3}$ λ'_+, λ''_+ and λ'_0 form factor parameters

Conclusion

K_{l3} form factors measurement is performed by NA48/2 experiment on the basis of 2004 run data. Result is competetive with the other ones in $K^{\pm}_{\mu 3}$, and a smallest error in $K^{\pm}_{e3}$ has been reached, that gives us also the combined result with the smallest error.

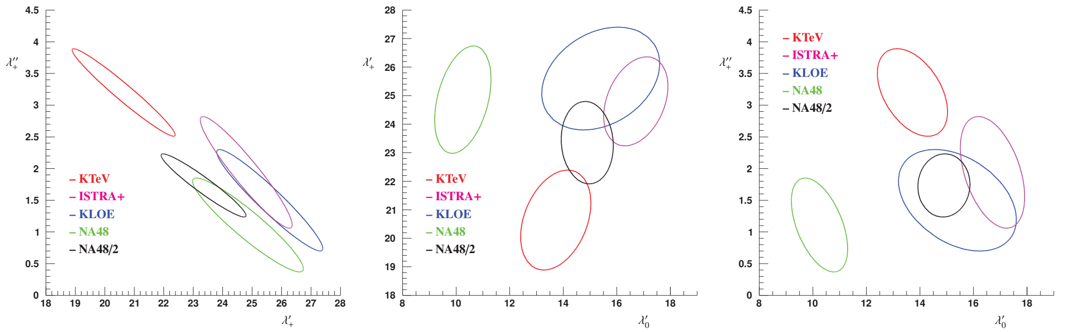

Figure 6. Joint K_{l3} results for the λ'_+, λ''_+ and λ'_0 form factor in comparison with the K_{l3} from another experiments [2].

References

[1] J.R. Batley et al. (NA48/2), Eur. Phys. J. **C52**, 875 (2007), 0707.0697
[2] M. Antonelli et al. (FlaviaNet Working Group on Kaon Decays), Eur.Phys.J. **C69**, 399 (2010), 1005.2323
[3] L.M. Chounet, J.M. Gaillard, M. Gaillard, Phys.Rept. **4**, 199 (1972)
[4] K. Olive et al. (Particle Data Group), Chin.Phys. **C38**, 090001 (2014)
[5] P. Lichard, Phys.Rev. **D55**, 5385 (1997), hep-ph/9702345
[6] V. Bernard, M. Oertel, E. Passemar, J. Stern, Phys.Rev. **D80**, 034034 (2009), 0903.1654
[7] V. Fanti et al. (NA48), Nucl. Instrum. Meth. **A574**, 433 (2007)
[8] G.D. Barr et al. (NA48), Nucl. Instrum. Meth. **A370**, 413 (1996)
[9] C. Patrignani et al. (Particle Data Group), Chin. Phys. **C40**, 100001 (2016)
[10] C. Gatti, Eur.Phys.J. **C45**, 417 (2006), hep-ph/0507280
[11] E.S. Ginsberg, Phys.Rev. **162**, 1570 (1967)
[12] F. James, M. Roos, Comput. Phys. Commun. **10**, 343 (1975)
[13] R. Brun, F. Rademakers, Nucl. Instrum. Meth. **A389**, 81 (1997)
[14] C. Amsler et al. (Particle Data Group), Phys.Lett. **B667**, 1 (2008)